Functional and molecular characterization of mouse Gata2-independent hematopoietic progenitors

Functional and molecular characterization of mouse Gata2-independent hematopoietic progenitors

Polynikis Kaimakis[1]*, Emma de Pater[1,4]*, Christina Eich[1]*, Parham Solaimani Kartalaei[1], Mari-Liis Kauts[1,2], Chris S. Vink[1,2], Reinier van der Linden[1], Martine Jaegle[1], Tomomasa Yokomizo[1], Dies Meijer[1,3] and Elaine Dzierzak[1,2]

[1]Erasmus MC Stem Cell Institute, Departments of Cell Biology and Genetics, Erasmus Medical Center, Rotterdam, Netherlands
[2]University of Edinburgh, Centre for Inflammation Research, Queens Medical Research Institute, Edinburgh, UK
[3]University of Edinburgh, Centre for NeuroRegeneration, Chancellor's Building, Edinburgh, UK
[4]Department of Hematology, Erasmus Medical Center, Rotterdam, Netherlands

*These authors contributed equally to this work.

Running title: Gata2-independent HPC

Abstract: 236
Text: 4002 words
Figures: 7
Tables: 3
Supplemental items: Methods, 1 Table, 1 Figure and Legend

Key words: Gata2; hematopoietic stem cells; HSC; AGM; development; hematopoiesis; hematopoietic progenitors; HPC; transgenic; Gata2 reporter; EHT; hemogenic endothelium; transcriptome

Corresponding author:
Elaine Dzierzak
University of Edinburgh
Centre for Inflammation Research
Queens Medical Research Institute
47 Little France Crescent
Edinburgh, EH16 4TJ
UK
Tel: +31 10 7043169
FAX: +31 10 7044743
Email: e.dzierzak@erasmusmc.nl
Elaine.Dzierzak@ed.ac.uk

Key Points

1. A new Gata2 reporter indicates that all HSCs express Gata2 and corroborates findings that Gata2 is not required for generation of all HPC.
2. Isolatable Gata2-non-expressing HPCs show less potency and a distinct genetic program, thus having implications for reprogramming strategies.

Abstract

The Gata2 transcription factor is a pivotal regulator of hematopoietic cell development and maintenance, highlighted by the fact that *Gata2* haploinsufficiency has been identified as the cause of some familial cases of AML/MDS and in MonoMac syndrome. Genetic deletion in mice has shown that Gata2 is pivotal to the embryonic generation of hematopoietic stem cells (HSC) and hematopoietic progenitor cells (HPC). It functions in the embryo during endothelial cell to hematopoietic cell transition (EHT) to affect hematopoietic cluster, HPC and HSC formation. *Gata2* conditional deletion and overexpression studies show the importance of Gata2 levels in hematopoiesis, during all developmental stages. Although previous studies of cell populations phenotypically enriched in HPCs and HSCs show expression of *Gata2*, there has been no direct study of Gata2 expressing cells during normal hematopoiesis. In this study we generate a *Gata2Venus* reporter mouse model with unperturbed Gata2 expression to examine the hematopoietic function and transcriptome of Gata2 expressing and non-expressing cells. We show that all the HSCs are Gata2 expressing. However, not all HPCs in the aorta, vitelline and umbilical arteries and fetal liver require or express Gata2. These Gata2-independent HPCs exhibit a different functional output and genetic program, including Ras and CREB pathways and other Gata factors, when compared to Gata2-dependent HPCs. Our results, indicating that Gata2 is of major importance in programming towards HSC fate but not in all cells with HPC fate, have implications for current reprogramming strategies.

Introduction

Gata2 is one of the 'heptad' transcription factors that acts on regulatory regions of hematopoietic genes[1]. It is upregulated *in vivo* in Ly6aGFP^{+} cells undergoing endothelial-to-hematopoietic cell transition (EHT), a process by which definitive hematopoietic progenitors (HPC) and HSCs are generated in the embryo[2,3]. As one of the major regulators of HPC and HSC generation, germline deficiency of *Gata2* results in embryonic lethality between E10-E10.5 and an anemic phenotype, with a decreased number of primitive and definitive HPCs in the yolk sac (YS) and in *Gata2*$^{-/-}$ ES cell hematopoietic differentiation cultures[4-6]. Chimeric embryo generation with *Gata2*$^{-/-}$ ES cells revealed defective production of all hematopoietic lineages[5]. The E10.5 lethality of *Gata2*$^{-/-}$ embryos precludes the study of HSC generation in the aorta-gonad-mesonephros (AGM) region, the first site of *de novo* HSC production. *Gata2*$^{+/-}$ embryos contain greatly reduced number of HSCs in the AGM region[7,8]. Gata2 haploinsufficiency perturbs adult HSC homeostasis in mouse[9], and in man leads to MonoMac syndrome[10], which is associated with sporadic myelodysplasia and myeloid leukemia. Also, rearrangement of the remote *Gata2* enhancer drives acute myeloid leukemogenesis by activating *Evi1* expression[11,12]. Overexpression studies also reveal that levels of Gata2 expression are important for its hematopoietic function[13-15]. *In situ* hybridization studies localize *Gata2* expression to aortic endothelial cells, intraaortic hematopoietic cluster cells, placenta (PL) and fetal liver (FL) in the midgestation mouse[16-18]. Conditional knockout of *Gata2* or *Gata2* regulatory elements in vascular endothelial cells indicates that Gata2 is essential for hematopoietic cluster formation and HSC generation[7,19,20]. Gata2 plays a role in the emergence of cKit-expressing hematopoietic cells from the endothelium[7]. Later, as shown in *VavCre* conditional knockout mice, *Gata2* is essential for HSC maintenance[7], thus demonstrating a role for Gata2 as previously recognized in bone marrow LSK HSCs[21].

To date, the correlation between Gata2 and hematopoietic cell generation in the embryo has been made in the absence of prospective isolation of viable Gata2-expressing cells[16]. Although some hematopoietic cells remain in the embryo in the absence of Gata2[5-8], the identity of these cells is unknown. In this study, to further understand the requirement for Gata2 in normal hematopoietic development, we create and use a mouse model in which a fluorescent reporter for Gata2 (*IRES-Venus* knock-in gene) does not affect the normal level or function of Gata2. We demonstrate that all long-term repopulating HSCs and a large percentage of HPCs in the midgestation mouse embryo are Venus-positive. We isolate and characterize a Venus-negative HPC population that corresponds to the HPCs found in *Gata2*-null embryos. Gata2-independent hematopoietic progenitors are functionally less complex and do not follow the same genetic program as Gata2-dependent HPCs.

Materials and methods

Gata2Venus ESC and mice. Generation of the Gata2-Venus mouse model is described in the online supplementary methods. In short, an *IRES-Venus* fragment and a *loxP-PGK-Puro-loxP* fragment were inserted in the *Gata2 3'UTR*. IB10 ESCs were transfected, puromycin-selected and 360 clones PCR screened for *Gata2Venus* (right arm junction 2292bp). Correct integration was verified by Southern blot (left arm) for 2 clones with normal karyotype. Founders were identified by *Venus* PCR. First generation *G2V* offspring were crossed with *CAG-Cre* mice[22] and backcrossed (>10 generations) with C57BL/6.

Mice and embryo production. Gata2$^{+/-}$ mice[5], Ly5.1(6-8 week) and C57BL/6 mice were obtained/maintained (Harlan or locally) and genotyped by PCR (online supplementary methods). Day of plug discovery is embryonic day (E)0. Embryos were staged by somite pair (sp): E9.5=16-28sp, E10=28-40sp, early E10=28-34sp, E10.5=35-40sp, E11=40-50sp.

Immunostaining. Whole-mount conceptuses were stained and imaged[23]; cryosections and flowcytometry were stained[8] using anti-CD34-biotin (1:50, BD), anti-Gata3 (1:10 KT122, 111207H09, Absea) and anti-Gata4 (1:50 H-112, sc-9053, SantaCruz) and anti-GFP antibodies. For flow cytometry[8], cells were stained with anti-CD31(390, BD), anti-CD34(RAM34, BD), anti-cKit(2B8, BD), anti-CD41(MWReg3, SantaCruz), anti-Sca1(D7, Ebiosciences) and anti-CD16/32(2.4G2, BD) antibodies, Hoechst 33258 (BD) and analysed (FACSARIAIII/SORP).

Hematopoietic assays. Venus-sorted E9-E11AGM, VA+UA, PL and YS and E10FL or *Gata2*-deficient E9-E10 AGM, VA+UA and PL were seeded in 3.6ml Methylcellulose (1ml per dish; M3434, StemCellTech) for 10-12 days[24]. Colonies were counted, isolated, washed and Venus expression examined (FACSARIAIII/Fortessa). Sorted *G2V* E11AGM (Ly5.1/Ly5.2) cells were transplanted[24] into 9.5Gy-irradiated (C57BL/6 x 129)F1 recipients (Ly5.2/Ly5.2) together with $2x10^5$ spleen cells from the recipient strain. Peripheral blood (PB) donor chimerism was determined by *Venus* PCR and/or FACS at 4mo post-transplantation and scored positive if PB donor chimerism was >10%.

RNA analyses. Detailed RNA procedures are provided in Online Supplemental Methods. GEO Data Accession Number is GSE76254. Briefly, RNA was isolated from E10.5 AGM CD31 and cKit sorted cells with mirVana miRNA Kit (Ambion) and quality/quantity assessed by 2100Bioanalyzer (Agilent; RNA Nano/Pico chip). RNAsequencing used SMARTER protocol for Illumina HiSeq2000 and analysed[25,26,27]. For qRT-PCR, SuperScriptII/III ReverseTranscriptase (LifeTechnologies) was used for first-strand cDNA synthesis. Primers are specified in Suppl Table1. *β-actin*=normalization control.

Results

Generation and validation of a novel *Gata2* reporter mouse model

Previously, analysis of *Gata2*-expressing cells has been limited to a reporter mouse model that results in Gata2 haploinsufficiency[16]. Our approach allows for the expression of the reporter within the *Gata2* genomic locus without affecting the levels of Gata2 expression or protein function. This is particularly important since Gata2 haploinsufficiency greatly reduces the number of HS/PCs generated during development[7,8,19,20,28]. Briefly, an internal ribosome entry site sequence (*IRES*) followed by the *Venus* fluorochrome gene was recombined into the *Gata2 3'UTR* (Fig1A) in embryonic stem cells (ESC). The resulting *Gata2Venus (G2V)* mice bred normally and showed no overt growth or hematopoietic defects.

To determine whether *Venus* reporter expression parallels that of *Gata2*, *G2V* bone marrow (BM) cells were sorted into Venus-expressing ($Venus^+$) and non-expressing ($Venus^-$) fractions (Fig1B). qRT-PCR for *Gata2* and *Venus* transcripts ($Gata2^{V/+}$ BM) demonstrated that only $Venus^+$ cells express *Venus* and *Gata2* mRNA (Fig1C). Western blot analysis revealed that equivalent amounts of Gata2 protein were present in $Gata2^{+/+}$ and $Gata2^{V/V}$ adult BM cells (data not shown). FACS analysis showed that $Gata2^{v/v}$ BM LSK cell numbers ($388/10^5$) are comparable to WT BM LSK numbers ($378/10^5$). Importantly, the results of competitive limiting dilution transplantation analyses of $Gata2^{V/V}$ and WT BM cells demonstrate that HSCs are qualitatively and quantitatively normal in this mouse model (Fig1D). Thus, Venus expression correctly reports Gata2 expression without interfering with its normal expression levels or function.

Gata2 is expressed in emerging aortic hematopoietic cluster cells and other embryonic hematopoietic tissues

Venus expression was examined in midgestation *G2V* hematopoietic tissues. Flow cytometry revealed that E9-E11 AGM, yolk sac (YS), PL and FL contained $Venus^+$ cells (Fig1E). At E9, 6.28%±0.47 of viable YS cells and 1.82%±0.31 of AGM cells are $Venus^+$. At E10.5 (when the first HSCs are generated) 3.27%±0.52 of AGM cells are $Venus^+$ and this increases to 19.27%±2.14 at E11. Table1 shows the frequencies of Gata2-expressing cells.

Whole mount images of E10 and E11 *G2V* embryos immunostained with anti-CD31 antibody (marks all endothelial cells and hematopoietic cluster cells) shows $Venus^+$ cells along the aorta (DA). $Venus^+$ cells are also observed in cells of the neural tube (NT), olfactory bulb (OB) and FL (Fig2A-C). In the E10.5 AGM region (DAPI- and CD31-stained (blue and red respectively)), Venus expression is found in endothelial and hematopoietic cluster cells mainly on the ventral side of the DA and in the urogenital (UG) region (Fig2D,E).

In the FL, Venus-expressing cells are found in a punctate distribution pattern (Fig2D,F). At E9, Venus is expressed in the some of the $CD34^+$ (red) endothelial cells of the paired aorta (Fig2G, arrowhead) and also in some of the endothelial and hematopoietic cluster cells of the umbilical artery (UA) (Fig2H). Venus continues to be expressed at E11 in some aortic endothelial cells, and emerging/other hematopoietic cluster cells (Fig2I, arrowhead). The E10.5 YS shows Venus expression in some of the $CD31^+$ (red) endothelial cells. Overall, Venus expression is similar to what has been previously documented for *Gata2 in situ* hybridization analysis[29,30]. Thus, our model allows for the prospective identification, isolation and characterization of Gata2-expressing cells during normal development.

All HSCs, but not all HPCs, express Gata2

To test for HSC activity, E11 AGM $Venus^+$ and $Venus^-$ cells were transplanted into irradiated adult recipients. All long-term repopulating HSCs were found in the Gata2Venus-expressing fraction (Fig3A). 9 of 19 recipients receiving $Venus^+$ cells were engrafted (15-71%), whereas none of 14 $Venus^-$ recipients showed donor-derived hematopoietic cells. These HSCs were multilineage-repopulating (Supplemental Fig1) and self-renewing (8 repopulated of 12 transplanted with $3x10^6$ BM cells from primary repopulated mice, n=4).

The relationship between Gata2 expression and HPC function was also examined. E9 and E10 AGM $Venus^+$ and $Venus^-$ cells were plated in the CFU-C assay. High enrichment of HPCs was found in the $Venus^+$ fractions (Table2). Surprisingly, HPCs were found also in the $Venus^-$ fraction, although there were very few. At E9 the $Venus^+$ and $Venus^-$ fractions respectively yielded 8.0±2.1 and 0.4±0.4 CFU-C per AGM. CFU-C numbers increased in the $Venus^+$ cell fraction at E10 (69.0±7.1), and the $Venus^-$ fraction increased to 8.0±2.3 CFU per AGM. However, bi- and multi-potent progenitors were found only in the $Venus^+$ fraction (Fig3B).

HPC activity was also examined in the $Venus^+$ and $Venus^-$ fractions of other hematopoietic tissues (Table2). E9 and E10 vitelline+umbilical arteries (VA+UA; Fig3C), YS (Fig3D) and PL (Fig3E), and E10 FL (Fig3F) contained progenitors in both fractions. Most HPCs were $Venus^+$. The greatest number of CFU-C arising from $Venus^-$ cells was found in the E9 YS (270.0±69.8 CFU-C/YS). These data indicate that some HPCs are not expressing Gata2. BFU-E, CFU-G and CFU-M were the predominant colony types in both fractions, and in contrast to the $Venus^+$ fractions, the $Venus^-$ fractions of VA+UA, YS, FL and PL yielded few or no CFU-GEMM. Thus, all AGM HSCs express Gata2, Gata2 expression is associated with immature HPCs, but not all HPCs are Gata2-expressing.

Some HPCs and vascular cluster cells are formed in the absence of *Gata2*

Since the $Venus^-$ fractions of midgestation *G2V* hematopoietic tissues contain CFU-C,

we tested whether such hematopoietic progenitors are present in *Gata2*-deleted embryos. CFU-Cs were detected in the *Gata2*$^{-/-}$ E9 AGM, E10 AGM (Fig4A) and E10 VA+UA (Fig4B), although significantly fewer as compared to WT (Table3). *Gata2*$^{+/-}$ tissues also contained fewer CFU-Cs compared to WT. The E9 *Gata2*$^{-/-}$ YS contained the most CFU-C (64.4±12.2)(Fig4C). In *VEC-Cre:Gata*$^{f/f}$ embryos, E10 PL showed significantly decreased CFU-C numbers (Fig4D), as did E10 AGM and YS[7] when compared to WT. The CFU-C remaining in *Gata2*$^{-/-}$ embryos are predominantly CFU-G and CFU-M. Very few *Gata2*$^{-/-}$ CFU-GM and no CFU-GEMM were observed. These data support and validate our findings in *G2V* embryos that not all HPCs are Gata2-expressing, Gata2-independent progenitors exist in each of the early hematopoietic tissues, and the Gata2-expressing cell fraction is more enriched in multipotent progenitors.

Since hematopoietic clusters appear in the VA and UA prior to appearance in the aorta, and are larger than in the AGM[31], we further examined these vessels. Whole-mount microscopic analysis demonstrates that clusters form in the absence of Gata2. The number and size of cKit^{+} hematopoietic clusters in early E10 *Gata2*$^{+/-}$ and *Gata2*$^{-/-}$ VA+UA are decreased as compared to WT(Fig4E). The number of cKit^{+} cells decreases 20-fold in the E10 *Gata2*$^{-/-}$ VA+UA (Fig4F) in correspondence to the decrease in VA+UA CFU-C (Fig4B), suggesting that these emerging cKit^{+} hematopoietic cluster cells are part of the cohort of Gata2-independent HPCs.

An alternative genetic program is expressed in Venus^{-} hematopoietic cells

The molecular basis for the functional differences observed in Gata2-dependent and -independent HPCs was examined by RNAsequencing. As most CD31^{+}Venus^{-} HPCs showed ckit intermediate (int) expression, we compared this population to CD31^{+}Venus^{+}ckit^{int} HPCs (Fig5A). Gene set enrichment analysis (GSEA) on genes sorted by log ratio of Venus^{+} versus Venus^{-} FPKMs revealed that genes in the Ras signalling pathway were significantly enriched in the Venus^{+} as compared to the Venus^{-} fraction (Fig5B). Genes upregulated by Ras were enriched in the Venus^{+} fraction, and highly upregulated genes included *Kras, Grb2* (Ras adaptor), and *Sos1* and *Sos2* (RasGEF activators) (Fig5C). Genes downregulated by Ras were enriched in the Venus^{-} fraction. RasGAP gene (render Ras inactive) *Rasa2* was highly-upregulated in the Venus^{-} fraction, whereas *Rasa1* and *Rasa3* were highly-upregulated in the Venus^{+} fraction. *Rasa4* and *NF1* were expressed to similar levels. Also, Venus^{+} HPCs show increased levels of *CREB* and *CBP* expression as compared to Venus^{-} HPCs, and express PKA catalytic subunit genes, suggesting that Venus^{+} HPCs have the potential to activate CREB target genes. *Gata2* has *CREB Response Element* consensus sites (-3kb,-300bp upstream tss) suggesting that it is a downstream target[32,33]. As *Gata2* is a Notch target[18], a 2-4-fold higher expression of *Notch1* and *Notch4* was found in the Venus^{+} fraction (Fig5D).

Moreover, *Snw1* and *Maml1* (transcriptional co-activators in the Notch pathway that interact with Notch) were upregulated (2- and 30-fold respectively) in Gata2-expressing HPCs.

Since Venus$^-$ HPCs are mainly restricted in their differentiation potential to the macrophage and granulocytic lineages, we evaluated their similarity to YS-derived erythromyeloid progenitors (EMPs) that give rise to tissue-resident macrophages. Flow cytometric analysis for EMP markers[34] showed that 3.89% of E10 YS and 0.72% of E10 AGM cells were EMPs (Sca1$^-$ckit$^+$CD41$^+$CD16/32$^+$). The majority of EMPs were Venus$^-$ (74% in YS, 85% in AGM) (Fig5F). At E11, the frequency of EMPs in the E11 YS and AGM decreased to 2.11% and 0.11% respectively (Fig5F), with 60% of YS and 77% of AGM EMPs now being Venus$^+$. Published transcriptome data on mouse YS EMPs show the low expression of several chemokine receptors/ligands (*Cx3cr1*, *Cx3cl1*, *Ccl2*, *Ccr1*, *Ccl9* and *Ccr7*)[35]. The expression of these genes was low or absent in Venus$^-$ AGM cells as compared to Venus$^+$ cells (Fig5F). Also, *Cxcr4* (highly-expressed in EMPs) was highly-expressed in Venus$^-$ AGM cells as compared to Venus$^+$ cells. These results suggest that the Venus$^-$ population shares similarities to EMPs at the transcription level.

Analysis of FPKMs for heptad transcription factors previously described as expressed in AGM HSCs and HPCs[1-3] showed expression in both the Venus$^+$ and Venus$^-$ AGM fractions (data not shown). Also, other Gata factors were expressed in both fractions. In the mouse *Gata1, 2* and *3* are hematopoietic transcription factors, whereas the *Gata4, 5* and *6* factors are not directly related to hematopoiesis. qRT-PCR performed on E10.5 AGM CD31$^+$cKit$^+$ cells (Fig6A) confirmed *Gata3* expression by both the Venus$^+$ and Venus$^-$ fractions, and *Gata4* was significantly higher in the Venus$^-$ fraction. *Gata1, 5, 6* transcripts were low/not detected. Immunostaining of E10.5 AGM (WT) showed Gata3-expressing cells in the mesenchyme underlying the ventral aspect of the aorta, aortic endothelial cells and some cells emerging from the aortic wall (Fig6B) in agreement with Fitch[36]. *G2V* E10.5 AGM confirmed that some aortic endothelial cells co-express Gata3 and Gata2(Fig6C). Gata4 expression was also found in aortic endothelial (CD34$^+$) cells, but it did not overlap with Gata2 expression(Fig6D). Together, these results suggest that Gata3 and/or Gata4 may provide some function in Gata2-independent hematopoietic cells.

Discussion

In this study we prospectively enriched and characterized Gata2-dependent and –independent HPC subsets from our novel *Gata2Venus* reporter mouse. Molecular analyses, together with the fact that some vascular hematopoietic cluster cells and HPCs persist in the absence of Gata2 expression suggest that an alternative genetic program exists for the production of HPCs. The transcriptome differences observed between Venus$^+$ and Venus$^-$ HPCs may offer possibilities for pathway modifications to achieve the programming

complexities necessary for the generation/function of normal definitive HPCs and provide insights into the factors involved in myeloid leukemogenesis.

Gata2 expression in the developing hematopoietic system

We showed the temporal and quantitatively coordinate transcription of *Venus* and *Gata2* in our *G2V* mouse model. The strategy used[37] eliminates expression level and protein alterations that affect HP/SC development. In *G2V* embryos, we showed that the cells with the most robust and complex hematopoietic potential (all HSCs and most HPCs) are Gata2-expressing. Imaging and FACS analyses of *G2V* embryos confirm that Gata2 is expressed in all hematopoietic sites during midgestation and that the numbers of Gata2-expressing cells reflect the developmental and temporal hematopoietic changes occurring in each site. At E9 Gata2-expressing cells are found predominantly in the YS, which at this time produces the highest numbers of the hematopoietic progenitors (EMP) in the conceptus. Slightly later as hematopoiesis begins in the AGM and FL, the numbers of Gata2-expressing cells also increase. The highest numbers of $CD31^{+}cKit^{+}$ cluster cells are found in the aorta, VA and UA at E10.5, as quantitated by whole mount embryo imaging[31]. Most, but not all hematopoietic cluster cells express Gata2, and *Gata2* expression may be downregulated as HPCs differentiate. However, we found some hematopoietic cluster cells and HPCs in the E10 *Gata2*$^{-/-}$ vasculature, confirming the existence of Gata2-independent HPCs[5].

Importantly, Gata2 is expressed in the endothelial cells of the DA. Already at E8.5, endothelial cells lining the paired dorsal aortae express Gata2 and it continues to be expressed in the E10.5 aorta when HSCs are generated, thus highlighting an involvement of Gata2 in the hemogenic program of endothelial cells. Data in *VE-cadherin* conditional *Gata2*-deficient mice and other models[7,19,28,38] strongly support the notion that Gata2 is required in hemogenic endothelium for the emergence of HSCs, as does the morpholino knockdown of *Gata2b* in Zebrafish[39].

Gata2 and the relationship with hematopoietic function

Prospective isolation and *in vivo* transplantation showed that all HSCs are Gata2-expressing. In contrast, some HPCs are present in the $Venus^{-}$ cell fractions of *G2V* hematopoietic tissues and *Gata2*$^{-/-}$ hematopoietic tissues. In both cases, the HPCs are restricted in their differentiation potential to predominantly the macrophage and granulocytic lineages. Currently, the EMP population is of high interest as a novel hematopoietic cell subset providing tissue resident macrophages[35,40-42]. Our FACS data revealed that EMPs are mainly in the $Venus^{-}$ cell population of E10 YS and AGM, and increased in the $Venus^{+}$ population at E11. Chemokine receptor/ligand gene sets obtained from a study on EMP/microglia transcriptome comparisons allowed us to find similarities in chemokine

receptor/ligand expression between EMPs and the Venus$^-$ HPC fraction.

Despite prevalence of EMPs in the Venus$^-$ cell population in E10 YS and AGM, definitive progenitors are largely Venus$^+$. The co-existence of these HPC subsets highlight the fact that there is more diversity in the types of progenitors generated in the embryo than was previously appreciated. In support of this is recent data from ESC hematopoietic differentiation cultures suggesting that there are two different hemogenic endothelial cell subsets[43] and the fact that *in vivo*, the AGM, VA/UA, YS, PL and head are all hemogenic tissues [34,44,45,46,47].

The highest number of Venus$^-$ HPCs were found in E9 and E10 YS (270.0±69.8 and 130.0±25.5 CFU-C, respectively) as compared to other tissues (PL, AGM, VA+UA). It is clear that Gata2 has an important role in EHT in the hemogenic endothelial cell compartment before or during the generation/emergence of hematopoietic cells, as evidenced by the decrease (but not absence) in the hematopoietic cluster cells in *Gata2*$^{-/-}$ aorta, VA and UA. However, it is as yet unclear at what frequency EHT occurs in the YS, thus raising the possibility that Gata2-independent HPCs arise differently than Gata2-dependent HPCs (perhaps directly from hemangioblasts[48]).

We found differences in the number of CFU from E9 YS Venus$^-$ cells (270.0±69) and Gata2$^{-/-}$ cells (64.4±12.2) (Fig4C,3D, Tables 2,3). The 4-fold lower CFU number is likely related to observations (ours and others) that colonies from *Gata2*$^{-/-}$ embryos, YS explants and ESC differentiations were smaller/less proliferative than WT colonies, due to the complete absence of Gata2[6,7]. Venus$^-$ cells are not defective for Gata2 and resulting colonies are normal in size. Whereas at the time of sorting they did not express Gata2, Gata2 expression could initiate after seeding Venus$^-$ HPCs in methylcellulose and cells thus undergo normal proliferation/differentiation. To test whether Venus$^-$ HPCs can convert to Venus$^+$ cells, we analysed Venus expression in colonies derived from sorted YS fractions after 10 days of differentiation (Fig7). Venus expression was found in colonies derived from both fractions, indicating that a portion of Venus$^-$ cells start to express Gata2 during formation of a hematopoietic colony. Interestingly, colonies derived from Venus$^+$ cells showed a Gr1$^+$ and Mac1$^+$ phenotype, whereas Venus$^-$ -derived colony cells were only Mac1$^+$. This demonstrates that Gata2 is not necessary for a subset of HPCs and that Gata2 promotes more complex hematopoietic function in other progenitor subsets.

Gata3/Gata4 redundancy in Gata2 independent progenitors

The expression of Gata3 and Gata4 in Venus$^-$ AGM HPCs and aortic endothelial cells is intriguing and highlights the potential redundancy of Gata transcription factors in hematopoietic cell generation. *Gata2* and *Gata3* can partially rescue the erythroid phenotype in *Gata1* deficient mice[49,50] and while recently it was suggested that *Gata3* is redundant in

HSCs[51], others clearly show that it regulates HSC cell-cycle entry[52] and self-renewal[53]. The fact that *Gata3* and *Gata4* are expressed in *Gata2*-non-expressing enriched HPCs suggests that they may function in this early progenitor subset. *Gata3*-deficient embryos show decreased numbers of FL HP/SCs[54]. Gata3 affects HSC development non-cell autonomously by activating the expression of *Th* (tyrosine hydroxylase) and hence, catecholamine production in the ventro-lateral cells of the sympathetic nervous system underlying the embryonic aorta[36]. HSC production was rescued when catecholamines were administered to the pregnant dams. These investigators also found that some aortic endothelial cells express a *Gata3LacZ* reporter, leaving open the possibility of a direct and overlapping role for Gata3 in some HPCs.

Much less is known concerning Gata4 in hematopoietic development. In Zebrafish there is a close relationship between anterior hemangioblasts and cardiac precursors[55]. Together with *Gata5* and *Gata6, Gata4* specifies these two anterior mesoderm derivatives. In mouse, *Gata4* is a key component of the cardiac developmental program, with close associations between cardiac, vascular and hematopoietic lineages[56-58]. Moreover, a subset of mouse endocardial and YS endothelial cells express cardiac markers, possess hemogenic potential and give rise to transient definitive erythroid/myeloid progenitors[59]. Our results suggest the Gata4 aortic endothelial cells and Venus$^-$ Gata4-expressing HPCs may be derivatives of mesodermal cells with a genetic program that retains cardiac-vascular-hematopoietic potential and can produce HPCs. Further examination of double reporter and deficient mice should reveal the overlapping and/or redundant roles of these Gata factors.

Gata2 as a pivotal regulator of complex hematopoietic function.

RNAsequence comparisons of the functionally distinct Venus$^+$ and Venus$^-$ HPC subsets revealed a strong upregulation of *Kras,* and *Ras* pathway genes, in Venus$^+$ HPCs. This pathway is particularly important in cell differentiation, acting as a molecular switch to relay extracellular growth signals[60]. *Kras* mutations confer a competitive-repopulating advantage to BM HSCs in transplantations and initiate leukemia in mice[61]. In human, *Kras* mutations (together with other cooperating gene mutations) are prevalent in patients with various forms of myelomonocytic and myeloid leukemia[62]. Interactions between oncogenic Ras and Gata2 have been proposed[63]. The normal function of Kras has not yet been explored fully. However, conditional deletion of *Kras* by *Vav-Cre* or *Mx1-Cre* does not affect HSCs or the adult hematopoietic system[64]. Yet chimeric mice, produced by *Kras*$^{-/-}$ ESC-blastocyst injection, show no contribution of *Kras*$^{-/-}$ cells to the hematopoietic system, suggesting that Kras may be important during the embryonic development of the hematopoietic system, but not after its generation.

The low expression of *Notch1*, *Notch4* and co-activators in the Venus$^-$ as compared to

the Venus$^+$ HPC fraction, supports the fact that early hematopoietic cells are generated independent of this signaling pathway, or implies that these are differentiated cells which have turned off Notch signalling[65]. Others have shown that *Notch1* deletion impairs the development of HSCs and angiogenesis[66], but not YS primitive or definitive hematopoiesis. Moreover, *Gata2* expression in the aortic endothelium is lost when *Jagged1* (ligand) is deleted[67]. Our data demonstrate a direct relationship for Notch and Gata2 expression, strongly supporting a pivotal role for this pathway in the generation of functionally-complex hematopoietic cells. In the absence of Notch signaling, less complex HPC emerge in the AGM or are immigrants from the YS[18,66,67]. In addition, our observed upregulated-expression of some CREB genes in Venus$^+$ HPCs supports the involvement of these regulators in definitive hematopoietic cell generation[68]. Our *Gata2Venus* model, in combination with recently reported *Gata2* distal enhancer-*Evi1* mouse model, will allow for a direct examination of the cells relevant to leukemogenesis[12].

In conclusion, we have enriched, localized and characterized Gata2-dependent and independent subsets of hematopoietic progenitors in *Gata2Venus* embryos. The combination of this reporter with other reporter and KO models will lead to a better understanding of the role of Gata2 (and other factors) in the development and function of multipotential HP/SCs in health, leukemogenesis and reprogramming.

Acknowledgements

We thank Prof Jim Palis for critical comments on this manuscript. Dr Dorota Kurek for providing anti-Gata3 and Gata4 antibodies; Drs Dorota Kurek and Mihaela Crisan for immunostaining support; Dr Siska Driegen for ESC culture support; Dr. Derk ten Berge for providing Wnt for ESC cultures. This work was supported by ZonMw (Dutch Medical Research Council 911-09-036), FES Netherlands Institute for Regenerative Medicine (101675), NIH (RO37 DK54077), ZonMW TOP (91211068), ERC Advanced Grant (341096) and LSBR (1344).

Authorship Contributions

PK, EdP, CE, MLK, MJ, CSV and TY performed research. PSK analysed RNAseq data. RvdL performed/analysed flow cytometric data. DM provided reagents. PK, EdP, CE, DM and ED designed experiments, analysed and interpreted data. PK, ED, EdP and CE wrote the manuscript.

Disclosure of Conflicts of Interest

The authors declare no conflicts of interest.

References

1. Wilson NK, Foster SD, Wang X, et al. Combinatorial transcriptional control in blood stem/progenitor cells: genome-wide analysis of ten major transcriptional regulators. *Cell Stem Cell*. 2010;7(4):532-544.
2. Solaimani Kartalaei P, Yamada-Inagawa T, Vink CS, et al. Whole-transcriptome analysis of endothelial to hematopoietic stem cell transition reveals a requirement for Gpr56 in HSC generation. *J Exp Med*. 2015;212(1):93-106.
3. Swiers G, Baumann C, O'Rourke J, et al. Early dynamic fate changes in haemogenic endothelium characterized at the single-cell level. *Nat Commun*. 2013;4:2924.
4. Fujiwara Y, Chang AN, Williams AM, Orkin SH. Functional overlap of GATA-1 and GATA-2 in primitive hematopoietic development. *Blood*. 2004;103(2):583-585.
5. Tsai FY, Keller G, Kuo FC, et al. An early haematopoietic defect in mice lacking the transcription factor GATA-2. *Nature*. 1994;371(6494):221-226.
6. Tsai FY, Orkin SH. Transcription factor GATA-2 is required for proliferation/survival of early hematopoietic cells and mast cell formation, but not for erythroid and myeloid terminal differentiation. *Blood*. 1997;89(10):3636-3643.
7. de Pater E, Kaimakis P, Vink CS, et al. Gata2 is required for HSC generation and survival. *J Exp Med*. 2013;210(13):2843-2850.
8. Ling KW, Ottersbach K, van Hamburg JP, et al. GATA-2 plays two functionally distinct roles during the ontogeny of hematopoietic stem cells. *J Exp Med*. 2004;200(7):871-882.
9. Rodrigues NP, Janzen V, Forkert R, et al. Haploinsufficiency of GATA-2 perturbs adult hematopoietic stem-cell homeostasis. *Blood*. 2005;106(2):477-484.
10. Hsu AP, Johnson KD, Falcone EL, et al. GATA2 haploinsufficiency caused by mutations in a conserved intronic element leads to MonoMAC syndrome. *Blood*. 2013;121(19):3830-3837, S3831-3837.
11. Groschel S, Sanders MA, Hoogenboezem R, et al. A single oncogenic enhancer rearrangement causes concomitant EVI1 and GATA2 deregulation in leukemia. *Cell*. 2014;157(2):369-381.
12. Yamazaki H, Suzuki M, Otsuki A, et al. A remote GATA2 hematopoietic enhancer drives leukemogenesis in inv(3)(q21;q26) by activating EVI1 expression. *Cancer Cell*. 2014;25(4):415-427.
13. Heyworth C, Gale K, Dexter M, May G, Enver T. A GATA-2/estrogen receptor chimera functions as a ligand-dependent negative regulator of self-renewal. *Genes Dev*. 1999;13(14):1847-1860.
14. Persons DA, Allay JA, Allay ER, et al. Enforced expression of the GATA-2 transcription factor blocks normal hematopoiesis. *Blood*. 1999;93(2):488-499.

15. Nandakumar SK, Johnson K, Throm SL, Pestina TI, Neale G, Persons DA. Low-level GATA2 overexpression promotes myeloid progenitor self-renewal and blocks lymphoid differentiation in mice. *Exp Hematol*. 2015;43(7):565-577 e510.
16. Minegishi N, Suzuki N, Yokomizo T, et al. Expression and domain-specific function of GATA-2 during differentiation of the hematopoietic precursor cells in midgestation mouse embryos. *Blood*. 2003;102(3):896-905.
17. Ottersbach K, Dzierzak E. Analysis of the mouse placenta as a hematopoietic stem cell niche. *Methods Mol Biol*. 2009;538:335-346.
18. Robert-Moreno A, Espinosa L, de la Pompa JL, Bigas A. RBPjkappa-dependent Notch function regulates Gata2 and is essential for the formation of intra-embryonic hematopoietic cells. *Development*. 2005;132(5):1117-1126.
19. Gao X, Johnson KD, Chang YI, et al. Gata2 cis-element is required for hematopoietic stem cell generation in the mammalian embryo. *J Exp Med*. 2013;210(13):2833-2842.
20. Lim KC, Hosoya T, Brandt W, et al. Conditional Gata2 inactivation results in HSC loss and lymphatic mispatterning. *J Clin Invest*. 2012;122(10):3705-3717.
21. Orlic D, Anderson S, Biesecker LG, Sorrentino BP, Bodine DM. Pluripotent hematopoietic stem cells contain high levels of mRNA for c-kit, GATA-2, p45 NF-E2, and c-myb and low levels or no mRNA for c-fms and the receptors for granulocyte colony-stimulating factor and interleukins 5 and 7. *Proc Natl Acad Sci U S A*. 1995;92(10):4601-4605.
22. Sakai K, Miyazaki J. A transgenic mouse line that retains Cre recombinase activity in mature oocytes irrespective of the cre transgene transmission. *Biochem Biophys Res Commun*. 1997;237(2):318-324.
23. Yokomizo T, Yamada-Inagawa T, Yzaguirre AD, Chen MJ, Speck NA, Dzierzak E. Whole-mount three-dimensional imaging of internally localized immunostained cells within mouse embryos. *Nat Protoc*. 2012;7(3):421-431.
24. Medvinsky A, Taoudi S, Mendes S, Dzierzak E. Analysis and manipulation of hematopoietic progenitor and stem cells from murine embryonic tissues. *Curr Protoc Stem Cell Biol*. 2008;Chapter 2:Unit 2A 6.
25. Trapnell C, Hendrickson DG, Sauvageau M, Goff L, Rinn JL, Pachter L. Differential analysis of gene regulation at transcript resolution with RNA-seq. *Nat Biotechnol*. 2013;31(1):46-53.
26. Mootha VK, Bunkenborg J, Olsen JV, et al. Integrated analysis of protein composition, tissue diversity, and gene regulation in mouse mitochondria. *Cell*. 2003;115(5):629-640.

27. Subramanian A, Tamayo P, Mootha VK, et al. Gene set enrichment analysis: a knowledge-based approach for interpreting genome-wide expression profiles. *Proc Natl Acad Sci U S A*. 2005;102(43):15545-15550.
28. Johnson KD, Hsu AP, Ryu MJ, et al. Cis-element mutated in GATA2-dependent immunodeficiency governs hematopoiesis and vascular integrity. *J Clin Invest*. 2012;122(10):3692-3704.
29. Nardelli J, Thiesson D, Fujiwara Y, Tsai FY, Orkin SH. Expression and genetic interaction of transcription factors GATA-2 and GATA-3 during development of the mouse central nervous system. *Dev Biol*. 1999;210(2):305-321.
30. Pimanda JE, Ottersbach K, Knezevic K, et al. Gata2, Fli1, and Scl form a recursively wired gene-regulatory circuit during early hematopoietic development. *Proc Natl Acad Sci U S A*. 2007;104(45):17692-17697.
31. Yokomizo T, Dzierzak E. Three-dimensional cartography of hematopoietic clusters in the vasculature of whole mouse embryos. *Development*. 2010;137(21):3651-3661.
32. Impey S, McCorkle SR, Cha-Molstad H, et al. Defining the CREB regulon: a genome-wide analysis of transcription factor regulatory regions. *Cell*. 2004;119(7):1041-1054.
33. Zhang X, Odom DT, Koo SH, et al. Genome-wide analysis of cAMP-response element binding protein occupancy, phosphorylation, and target gene activation in human tissues. *Proc Natl Acad Sci U S A*. 2005;102(12):4459-4464.
34. McGrath KE, Frame JM, Fegan KH, et al. Distinct Sources of Hematopoietic Progenitors Emerge before HSCs and Provide Functional Blood Cells in the Mammalian Embryo. *Cell Rep*. 2015;11(12):1892-1904.
35. Kierdorf K, Erny D, Goldmann T, et al. Microglia emerge from erythromyeloid precursors via Pu.1- and Irf8-dependent pathways. *Nat Neurosci*. 2013;16(3):273-280.
36. Fitch SR, Kimber GM, Wilson NK, et al. Signaling from the sympathetic nervous system regulates hematopoietic stem cell emergence during embryogenesis. *Cell Stem Cell*. 2012;11(4):554-566.
37. Nutt SL, Metcalf D, D'Amico A, Polli M, Wu L. Dynamic regulation of PU.1 expression in multipotent hematopoietic progenitors. *J Exp Med*. 2005;201(2):221-231.
38. Khandekar M, Brandt W, Zhou Y, et al. A Gata2 intronic enhancer confers its pan-endothelia-specific regulation. *Development*. 2007;134(9):1703-1712.
39. Butko E, Distel M, Pouget C, et al. Gata2b is a restricted early regulator of hemogenic endothelium in the zebrafish embryo. *Development*. 2015;142(6):1050-1061.
40. Ginhoux F, Greter M, Leboeuf M, et al. Fate mapping analysis reveals that adult microglia derive from primitive macrophages. *Science*. 2010;330(6005):841-845.

41. Gomez Perdiguero E, Klapproth K, Schulz C, et al. Tissue-resident macrophages originate from yolk-sac-derived erythro-myeloid progenitors. *Nature*. 2015;518(7540):547-551.
42. Herbomel P, Thisse B, Thisse C. Zebrafish early macrophages colonize cephalic mesenchyme and developing brain, retina, and epidermis through a M-CSF receptor-dependent invasive process. *Dev Biol*. 2001;238(2):274-288.
43. Ditadi A, Sturgeon CM, Tober J, et al. Human definitive haemogenic endothelium and arterial vascular endothelium represent distinct lineages. *Nat Cell Biol*. 2015;17(5):580-591.
44. Palis J, Yoder MC. Yolk-sac hematopoiesis: the first blood cells of mouse and man. *Exp Hematol*. 2001;29(8):927-936.
45. Frame JM, McGrath KE, Palis J. Erythro-myeloid progenitors: "definitive" hematopoiesis in the conceptus prior to the emergence of hematopoietic stem cells. *Blood Cells Mol Dis*. 2013;51(4):220-225.
46. Lux CT, Yoshimoto M, McGrath K, Conway SJ, Palis J, Yoder MC. All primitive and definitive hematopoietic progenitor cells emerging before E10 in the mouse embryo are products of the yolk sac. *Blood*. 2008;111(7):3435-3438.
47. Rhodes KE, Gekas C, Wang Y, et al. The emergence of hematopoietic stem cells is initiated in the placental vasculature in the absence of circulation. *Cell Stem Cell*. 2008;2(3):252-263.
48. Jaffredo T, Nottingham W, Liddiard K, Bollerot K, Pouget C, de Bruijn M. From hemangioblast to hematopoietic stem cell: an endothelial connection? *Exp Hematol*. 2005;33(9):1029-1040.
49. Takahashi S, Shimizu R, Suwabe N, et al. GATA factor transgenes under GATA-1 locus control rescue germline GATA-1 mutant deficiencies. *Blood*. 2000;96(3):910-916.
50. Tsai FY, Browne CP, Orkin SH. Knock-in mutation of transcription factor GATA-3 into the GATA-1 locus: partial rescue of GATA-1 loss of function in erythroid cells. *Dev Biol*. 1998;196(2):218-227.
51. Buza-Vidas N, Duarte S, Luc S, Bouriez-Jones T, Woll PS, Jacobsen SE. GATA3 is redundant for maintenance and self-renewal of hematopoietic stem cells. *Blood*. 2011;118(5):1291-1293.
52. Ku CJ, Hosoya T, Maillard I, Engel JD. GATA-3 regulates hematopoietic stem cell maintenance and cell-cycle entry. *Blood*. 2012;119(10):2242-2251.
53. Frelin C, Herrington R, Janmohamed S, et al. GATA-3 regulates the self-renewal of long-term hematopoietic stem cells. *Nat Immunol*. 2013;14(10):1037-1044.
54. Pandolfi PP, Roth ME, Karis A, et al. Targeted disruption of the GATA3 gene causes severe abnormalities in the nervous system and in fetal liver haematopoiesis. *Nat Genet*. 1995;11(1):40-44.

55. Peterkin T, Gibson A, Patient R. Common genetic control of haemangioblast and cardiac development in zebrafish. *Development*. 2009;136(9):1465-1474.
56. Fehling HJ, Lacaud G, Kubo A, et al. Tracking mesoderm induction and its specification to the hemangioblast during embryonic stem cell differentiation. *Development*. 2003;130(17):4217-4227.
57. Huber TL, Kouskoff V, Fehling HJ, Palis J, Keller G. Haemangioblast commitment is initiated in the primitive streak of the mouse embryo. *Nature*. 2004;432(7017):625-630.
58. Van Handel B, Montel-Hagen A, Sasidharan R, et al. Scl represses cardiomyogenesis in prospective hemogenic endothelium and endocardium. *Cell*. 2012;150(3):590-605.
59. Nakano H, Liu X, Arshi A, et al. Haemogenic endocardium contributes to transient definitive haematopoiesis. *Nat Commun*. 2013;4:1564.
60. Pierre S, Bats AS, Chevallier A, et al. Induction of the Ras activator Son of Sevenless 1 by environmental pollutants mediates their effects on cellular proliferation. *Biochem Pharmacol*. 2011;81(2):304-313.
61. Sabnis AJ, Cheung LS, Dail M, et al. Oncogenic Kras initiates leukemia in hematopoietic stem cells. *PLoS Biol*. 2009;7(3):e59.
62. Chang YI, You X, Kong G, et al. Loss of Dnmt3a and endogenous Kras cooperate to regulate hematopoietic stem and progenitor cell functions in leukemogenesis. *Leukemia*. 2015.
63. Katsumura KR, Yang C, Boyer ME, Li L, Bresnick EH. Molecular basis of crosstalk between oncogenic Ras and the master regulator of hematopoiesis GATA-2. *EMBO Rep*. 2014;15(9):938-947.
64. Kong G, Liu Y, Chang Y-I, Zhang J, Chang Q, Zhang J. Kras Plays An Important Role In Generating Differentiated Blood Cells. Vol. 122; 2013.
65. Richard C, Drevon C, Canto PY, et al. Endothelio-mesenchymal interaction controls runx1 expression and modulates the notch pathway to initiate aortic hematopoiesis. *Dev Cell*. 2013;24(6):600-611.
66. Kumano K, Chiba S, Kunisato A, et al. Notch1 but not Notch2 is essential for generating hematopoietic stem cells from endothelial cells. *Immunity*. 2003;18(5):699-711.
67. Robert-Moreno A, Guiu J, Ruiz-Herguido C, et al. Impaired embryonic haematopoiesis yet normal arterial development in the absence of the Notch ligand Jagged1. *EMBO J*. 2008;27(13):1886-1895.
68. Kim PG, Nakano H, Das PP, et al. Flow-induced protein kinase A-CREB pathway acts via BMP signaling to promote HSC emergence. *J Exp Med*. 2015;212(5):633-648.

Table 1. Frequency of Venus$^+$ cells in embryonic tissues of *G2V* embryos.

Tissue	Stage	(number of experiments, embryos analyzed)	% Venus+ cells/tissue
AGM	E9, 16-25sp	(n=4, 22)	1.82 ± 0.31
	E10, 28-36sp	(n=4, 29)	3.27 ± 0.52
	E11, 43-49sp	(n=4, 25)	7.86 ± 1.1
FL	E9	nd	nd
	E10, 28-36sp	(n=4, 10)	13.89 ± 0.7
	E11, 43-49sp	(n=4, 19)	19.27 ± 2.14
YS	E9, 16-25sp	(n=5, 8)	6.28 ± 0.47
	E10, 28-36sp	(n=6, 9)	6.17 ± 0.86
	E11, 42-46sp	(n=1, 3)	5.25 ± 0.59
PL	E9, 17-23sp	(n=3, 4)	10.91 ± 0.49
	E10, 28-35sp	(n=3, 6)	10.8 ± 1.92
	E11, 42-46sp	(n=1, 3)	15.01 ± 4.64

The frequency of Venus positive cells within the viable cell fraction of embryonic tissues per embryo is presented. FACS analysis of single cell suspensions of dissected embryonic tissues (YS, yolk sac; PL, placenta; AGM, aorta-gonads-mesonephros; FL, fetal liver) was performed to define the percentage of cells expressing Venus. AGM contains part of the vitelline and umbilical arteries. Our data for the total number of cells in each tissue (data not shown) correlated with published data for YS and E9.5 AGM (Dzierzak and de Bruijn 2002) and for FL (Gekas, Dieterlen-Lievre et al. 2005). The data represents the mean ± SEM of 3-6 independent experiments with exception of E11 YS and PL data (data represents the mean ± STD of 1 experiment. (n=number of independent experiments, number of individual embryos analysed), E=embryonic day, sp=somite pairs; nd=not done.

Table 2. CFU-C number in Venus$^+$ and Venus$^-$ cell fractions of *G2V* embryonic tissues

Tissue	Stage	(number of experiments, embryos analyzed)	CFU-C/tissue/sorted cell fraction	
			Venus$^-$	**Venus$^+$**
AGM	E9, 20-23sp	(n=2, 5)	0.4 ± 0.4	8.0 ± 2.1
	E10, 32-35sp	(n=2, 6)	8.0 ± 2.3	69.0 ± 7.1
VA+UA	E9, 20-23sp	(n=2, 5)	0.8 ± 0.5	2.4 ± 1.0
	E10, 32-35sp	(n=2, 6)	7.0 ± 1.5	197.7 ± 36.9
YS	E9, 20-23sp	(n=2, 5)	270.0 ± 69.8	1020 ± 137.3
	E10, 32-35sp	(n=2, 5)	130.0 ± 25.5	1252.0 ± 156.0
PL	E9, 20-23sp	(n=2, 5)	4.0 ± 1.3	22.0 ± 2.5
	E10, 32-35sp	(n=2, 6)	14.5 ± 5.3	251.7 ± 32.4
FL	E10, 32-35sp	(n=2, 6)	20.5 ± 7.6	248.7 ± 75.2

Number of total CFU-C (mean ± SEM) per tissue per *G2V* embryo for the sorted Venus$^-$ and Venus$^+$ cell fractions at E9 and E10. E=embryonic day, sp=somite pair. (n=number of independent experiments, number of individual embryos analysed).

Table 3. CFU-C number per E9-E10 *Gata2*-deleted hematopoietic tissues.

Tissue	Stage	Genotype					
		WT		***Gata2*$^{+/-}$**		***Gata2*$^{-/-}$**	
AGM	E9, 20-23sp	8.5 ± 2.3	(n=1, 4)	2.25 ± 0.9*	(n=1, 4)	3.0 ± 1.0	(n=1, 2)
	E10, 28-34sp	62.4 ± 20.8	(n=3, 7)	24.0 ± 7.4*	(n=3, 13)	16.7 ± 6.8*	(n=3, 9)
VA+UA	E9, 20-23sp	7.0 ± 0.6	(n=1, 4)	2.25 ± 0.6*	(n=1, 4)	5.0 ± 2.0	(n=1, 2)
	E10, 28-34sp	241.1 ± 67.8	(n=3, 7)	78.7 ± 12.3**	(n=3, 13)	12.0 ± 2.5**	(n=3, 9)
YS	E9, 20-23sp	772.5 ± 85.3	(n=1, 4)	500.0 ± 71.5*	(n=1, 4)	64.4 ± 12.2**	(n=1, 2)
	E10, 28-34sp	918.6 ± 147.9	(n=3, 7)	584.6 ± 89.0**	(n=3, 9)	25.7 ± 8.0**	(n=2, 3)
		***Gata2*$^{f/+}$ *or* *Gata2*$^{f/f}$**		***VEC-Cre:Gata2*$^{f/+}$**		***VEC-Cre:Gata2*$^{-/-}$**	
FL	E10, 30-34sp	115.8 ± 35.0	(n=2, 5)	83.0 ± 20.8	(n=2, 6)	22.2 ± 6.7*	(n=2, 6)
PL	E10, 30-34sp	406.0 ± 134.0	(n=2, 5)	81.0 ± 25.0*	(n=2, 6)	12.0 ± 4.0*	(n=2, 6)

Number of total CFU-C (mean ± SEM) per tissue shown for WT, *Gata2* germline and conditional knockout embryos at E9 and E10. WT=wild type, E=embryonic day, sp=somite pair, (n=number of independent experiments, number of individual embryos analysed), *$p < 0.05$; **$p < 0.01$

Figure Legends

Figure 1. Gata2 Venus reporter construction and validation. (A) Schematic diagram of the *IRES Venus* reporter-selection cassette insertion in the 3'UTR of the mouse *Gata2* locus and Cre-mediated removal of *lox PGK-Puro lox*. Primers used for detection of the targeted and recombined alleles are indicated flanking the loxP sites (yellow). (B) Representative flow cytometric analysis and sorting plot of Venus-expressing cells in the bone marrow (BM) of adult *Gata2 Venus* (*G2V*) mice. Gated regions show percentage positive and negative viable cells. (C) Relative levels of *Gata2* and *Venus* mRNA in sorted $Venus^+$ and $Venus^-$ $Gata2^{V/+}$ cells BM cells as determined by qRT-PCR. *Gata2* transcripts in $Venus^+$ cells=0.11337±0.00681 and $Venus^-$ cells=0.00012±0.00003, p=0.000076. *Venus* transcripts in $Venus^+$ cells=0.06722±0.00799 and $Venus^-$ cells=0.00036±0.00010, p=0.00112. mean ± SEM, n=3. (D) Competitive limiting dilution transplantation strategy used to test the quantity and robustness of $Gata2^{V/V}$ BM HSCs as compared to wild type. Percentage of donor cell chimerism in adult irradiated recipients co-transplanted with the same number of wild type (WT) Ly5.1/5.2 and *Gata2 Venus* ($G2^{V/V}$) Ly5.2 bone marrow cells. Varying numbers ($1x10^5$, $3x10^5$, $3x10^6$) of bone marrow cells of each genotype were injected and peripheral blood of recipients was analysed for donor cell engraftment by FACS at 1 and 4 months post transplantation. n=2 (5 mice per group). (E) Representative FACS plots demonstrating frequency of Venus expressing cells in E11 AGM, YS, PL and FL. Gates indicate $Venus^-$ and $Venus^+$ cell fractions. Percentages represent the frequency of $Venus^+$ cells within the viable cell fraction (See Table 1).

Figure 2. Localization of Gata2Venus expressing cells in embryonic hematopoietic sites. Confocal images of a whole mount immunostained E10.5 Gata2Venus embryo showing (A) Venus; green, (B) CD31; magenta and (C) merged expression. Venus expressing cells are detected in the aorta-gonad-mesonephros (AGM) along the wall of the dorsal aorta (dotted lines), the fetal liver (FL), neural tube (NT) and olfactory bulb (OB). (D) Confocal image of a transverse section through the E10.5 AGM. DAPI staining (blue), CD31 (red) and Venus fluorescence (green) reveal Gata2-expressing aortic endothelial and hematopoietic cluster cells, urogenital (UG) and liver (FL) cells. Enlarged images of panel D showing Gata2-expressing cells in (E) AGM (DA=dorsal aorta; UG=uro-genital ridges; arrowheads indicate hematopoietic cluster) and (F) FL. Venus (green) and CD34 (red) fluorescence showing endothelial and hematopoietic cluster cells in (G) E9 paired aorta (H) umbilical artery (UA) at E9 and (I) E11 aorta. Arrowheads indicate hematopoietic cluster. (J-M) Images of E10.5 yolk sac (YS) section showing DAPI merged, Venus, CD31 and merged fluorescence. Arrow denotes an endothelial cell expressing Venus and CD31.

Figure 3. Quantitation of functional HSCs and HPCs in *G2V* embryonic hematopoietic tissues. HSCs in sorted Venus$^+$ and Venus$^-$ cell fractions of E11 AGM were analysed by transplantation into irradiate adult recipients. (A) Percentage donor cell chimerism was determined by Venus PCR of peripheral blood DNA at 4 months post-transplantation. Each dot represents one recipient receiving 1.7-6.5 ee of AGM cells. n=7. **p=0.0089. (B-G) Hematopoietic progenitor number per tissue in sorted Venus$^+$ and Venus$^-$ cell fractions of (B) E9 and E10 AGM, (C) E9 and E10 VA+UA, (D) E9 and E10 yolk sac (YS), E9 and E10 placenta (PL), and (F) E10 fetal liver (FL). Colony forming unit–culture (CFU-C) per one ee of tissue is shown. Colony types designated by colored bars are CFU-granulocyte, erythroid, macrophage, megakaryocyte (GEMM); CFU-granulocyte, macrophage (GM); CFU-macrophage (M); CFU-granulocyte (G) and Burst forming unit-erythroid (BFU-E). SEM of total CFU-C is shown. 2 ee of somite pair matched tissues were pooled for sorting and yielded 1ee for colony analysis.

Figure 4. CFU-C numbers and vascular hematopoietic clusters in Gata2$^{-/-}$ embryos. CFU-C numbers per embryo equivalent (ee) found in (A) E9 and E10 AGM, (B) E9 and E10 VA+UA, (C) E9 and E10 YS, (D) E10 placenta. *p<0.05; **p<0.01. (E) Quantitation of cKit$^+$ hematopoietic cluster cells in VA+UA of E10 *Gata2*$^{+/+}$, *Gata2*$^{+/-}$ and *Gata2*$^{-/-}$ embryos. (F) Representative whole mount images of hematopoietic cluster cells in the VA of E10 *Gata2*$^{+/+}$ (30 sp), *Gata2*$^{+/-}$ (31 sp) and *Gata2*$^{-/-}$ (30 sp) embryos stained for cKit expression.

Figure 5. Differential expression of signalling pathway modulators in Gata2 dependent and independent HPCs. (A) Flow cytometric sorting gates for isolation of E10.5 AGM *G2V* CD31$^+$cKit^{int}Venus$^-$ (grey) and CD31$^+$cKit^{int}Venus$^-$ (green) HPCs used for RNA sequence analysis. GEO Data Accession Number is GSE76254. (B) Gene enrichment analysis for Ras signaling pathway genes. Bar graphs of FPKM values obtained from RNA sequence analysis of CD31$^+$cKit^{int}Venus$^-$ (grey bar) and CD31$^+$cKit^{int}Venus$^+$ (green bar) AGM cells for (C) Ras pathway and CREB and CBP transcription factor genes and (D) Notch pathway genes. (E) Bar graphs of FPKM values obtained from RNA sequence analysis for a selection of chemokine receptor/ligand genes (see Kiedorf et al, 2013; these genes were down-/upregulated in YS EMPs as compared to adult microglia (AM)). (F) Representative FACS plots demonstrating frequency of EMPs in the Venus$^+$ fraction, as defined as Sca1$^-$ ckit$^+$CD41$^+$CD16/32$^+$, in YS and AGM of E10 (left) and E11 (right) *G2V* embryos. Numbers indicate the percentages of gated cells within the parental cell population.

Figure 6. Gata family gene expression in AGM Gata2 dependent and independent

HPCs. (A) qRT-PCR for expression of *Gata1, 2, 3, 4, 5 and 6* transcription factors (normalization with *Gapdh*) in E11 AGM $CD31^{+}cKit^{+}Venus^{+}$ and $CD31^{+}cKit^{+}Venus^{-}$ cells. n=3. SEM shown with *p=0.05 and ***p=0.001 (B) Transverse section of WT E10.5 AGM immunostained for CD34 (magenta) and Gata3 (green) showing expression of Gata3 in the aortic endothelial cells and some emerging hematopoietic cells and ventral mesenchymal cells directly under the aorta. (C) Transverse section of *G2V* E10.5 AGM immunostained for CD34 (magenta), Gata2 (green) and Gata3 (red) showing some overlapping expression of Gata2 and Gata3 in aortic endothelial cells (arrowheads). (D) Transverse consecutive sections of E11 *G2V* AGM immunostained for CD34 (magenta) and Venus (green) in the top panels and for CD34 (magenta) and Gata4 (red) in the bottom panels. Gata4 expression is observed in some ventral aortic endothelial cells and emerging hematopoietic cells (arrow).

Figure 7. Gata2 is expressed by $Venus^{-}$ cells after culture. Schematic diagram showing method and FACS analysis by which Gata2 expression was found in the progeny of sorted $Venus^{-}$ HPCs. *G2V* YS tissue was FACS sorted into $Venus^{-}$ and $Venus^{+}$ fractions. Cells were subsequently seeded in methylcellulose and colonies analysed after 10 days of culture. Colonies were harvested from the dish and cells are washed, stained (with anti-Gr1 and anit-Mac1 antibodies) and Venus, Gr1 and Mac1 expression was analysed by FACS. FACS plots (top) indicate Venus expression in cells harvested from $Venus^{-}$ (left) and $Venus^{+}$ (right) CFU-C experiments. Note that both FACS analyses indicate Venus expression in both cultures. FACS plots (bottom) show Gr1 and Mac1 expression in $Venus^{-}$ and $Venus^{+}$ populations in both cultures, and that cells harvested from $Venus^{+}$ culture show a more immature phenotype.

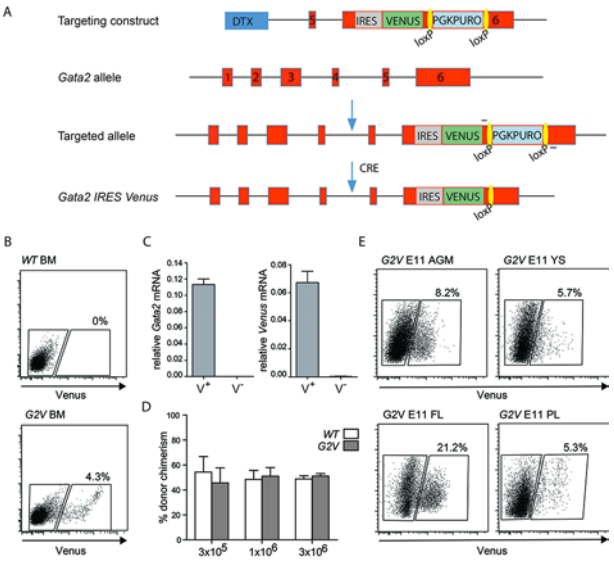
A
Targeting construct
DTX
IRES
VENUS
PGKPURO
6
loxP
loxP
Gata2 allele
1
2
3
4
5
6
Targeted allele
CRE
Gata2 IRES Venus
B
WT BM
0%
Venus
G2V BM
4.3%
Venus
C
relative Gata2 mRNA
relative Venus mRNA
V+
V-
D
% donor chimerism
WT
G2V
3x10^5
1x10^6
3x10^6
E
G2V E11 AGM
8.2%
G2V E11 YS
5.7%
Venus
G2V E11 FL
21.2%
G2V E11 PL
5.3%
Venus

Figure 1

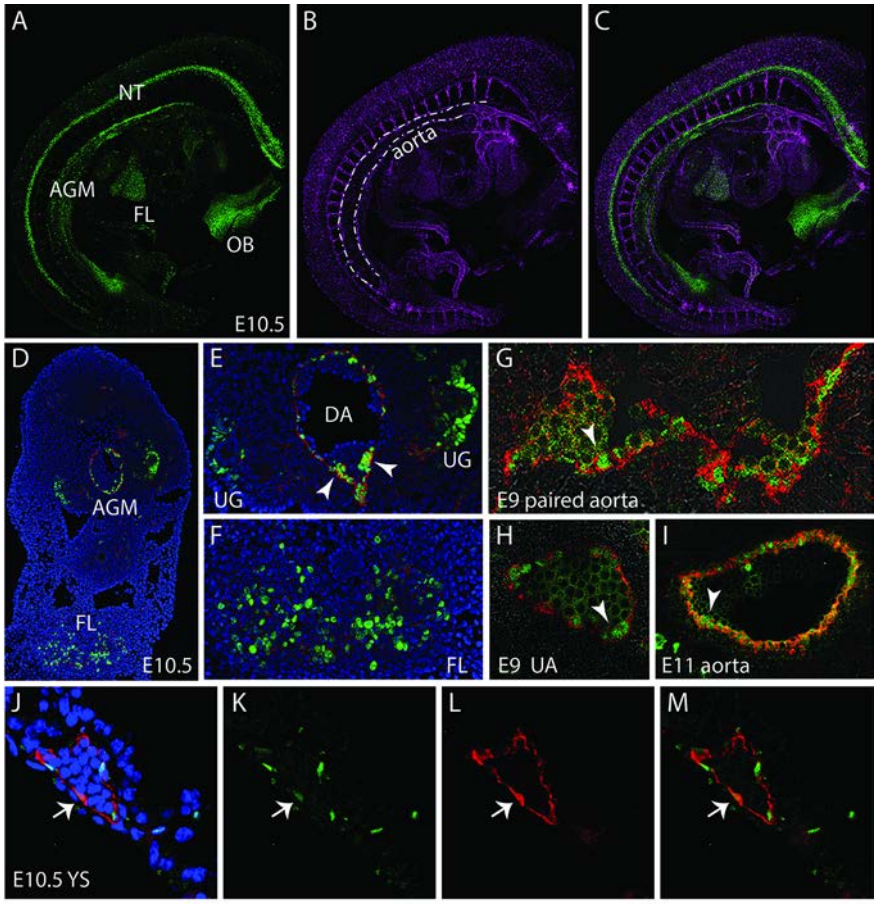
A
NT
AGM
FL
OB
E10.5
B
aorta
C
D
AGM
FL
E10.5
E
DA
UG
UG
G
E9 paired aorta
F
FL
H
E9 UA
I
E11 aorta
J
E10.5 YS
K
L
M

Figure 2

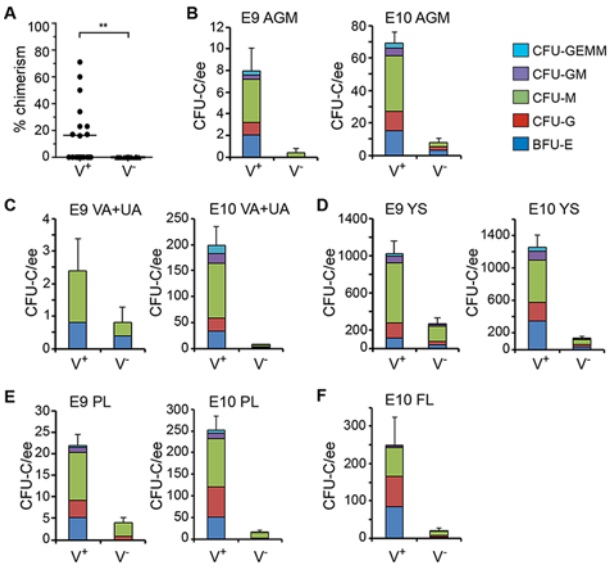
A
% chimerism
**
V+
V-
B
E9 AGM
E10 AGM
CFU-C/ee
CFU-GEMM
CFU-GM
CFU-M
CFU-G
BFU-E
C
E9 VA+UA
E10 VA+UA
D
E9 YS
E10 YS
E
E9 PL
E10 PL
F
E10 FL

Figure 3

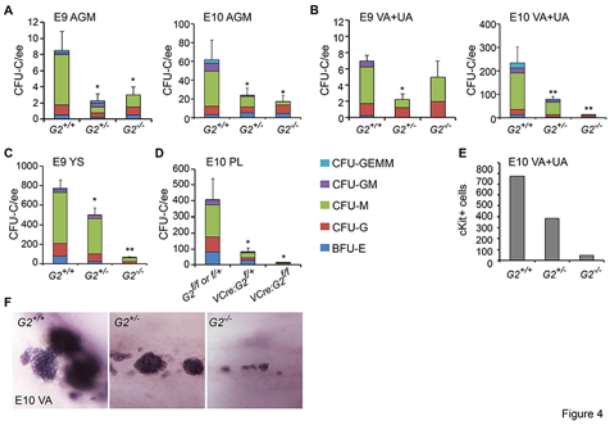
A
E9 AGM
E10 AGM
B
E9 VA+UA
E10 VA+UA
CFU-C/ee
C
E9 YS
D
E10 PL
CFU-GEMM
CFU-GM
CFU-M
CFU-G
BFU-E
E
E10 VA+UA
cKit+ cells
F
E10 VA

Figure 4

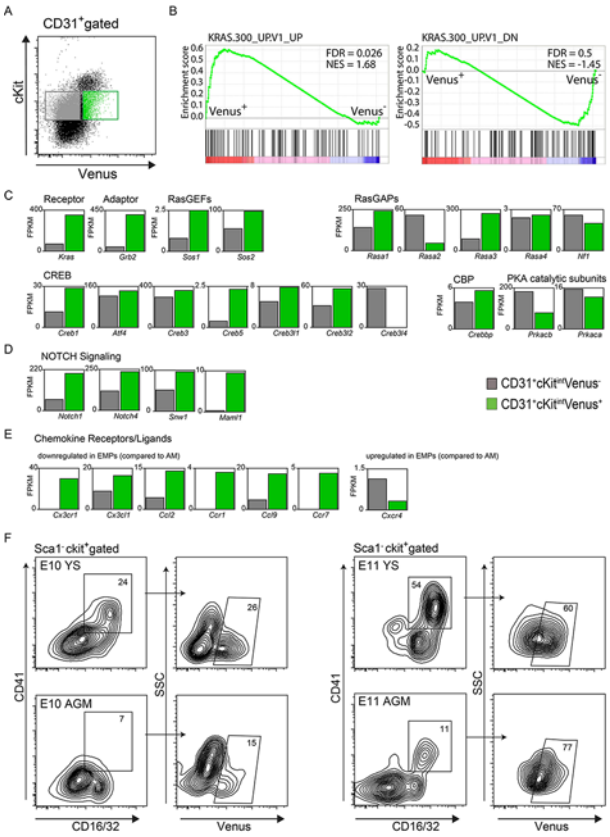
A
CD31+gated
cKit
Venus
B
KRAS.300_UP.V1_UP
FDR = 0.026
NES = 1.68
Enrichment score
Venus+
Venus-
KRAS.300_UP.V1_DN
FDR = 0.5
NES = -1.45
C
Receptor
Adaptor
RasGEFs
RasGAPs
Kras
Grb2
Sos1
Sos2
Rasa1
Rasa2
Rasa3
Rasa4
Nf1
CREB
Creb1
Atf4
Creb3
Creb5
Creb3l1
Creb3l2
Creb3l4
CBP
Crebbp
PKA catalytic subunits
Prkacb
Prkaca
D
NOTCH Signaling
Notch1
Notch4
Snw1
Maml1
CD31+cKitintVenus-
CD31+cKitintVenus+
E
Chemokine Receptors/Ligands
downregulated in EMPs (compared to AM)
upregulated in EMPs (compared to AM)
Cx3cr1
Cx3cl1
Ccl2
Ccr1
Ccl9
Ccr7
Cxcr4
F
Sca1-ckit+gated
E10 YS
E11 YS
E10 AGM
E11 AGM
CD41
SSC
CD16/32
Venus

Figure 5

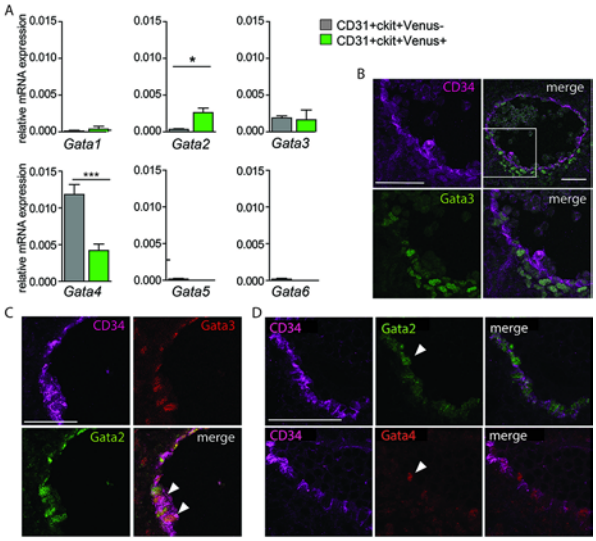
A
relative mRNA expression
0.015
0.010
0.005
0.000
Gata1
Gata2
Gata3
Gata4
Gata5
Gata6
*
***
CD31+ckit+Venus-
CD31+ckit+Venus+
B
CD34
merge
Gata3
C
Gata2
D
Gata4

Figure 6

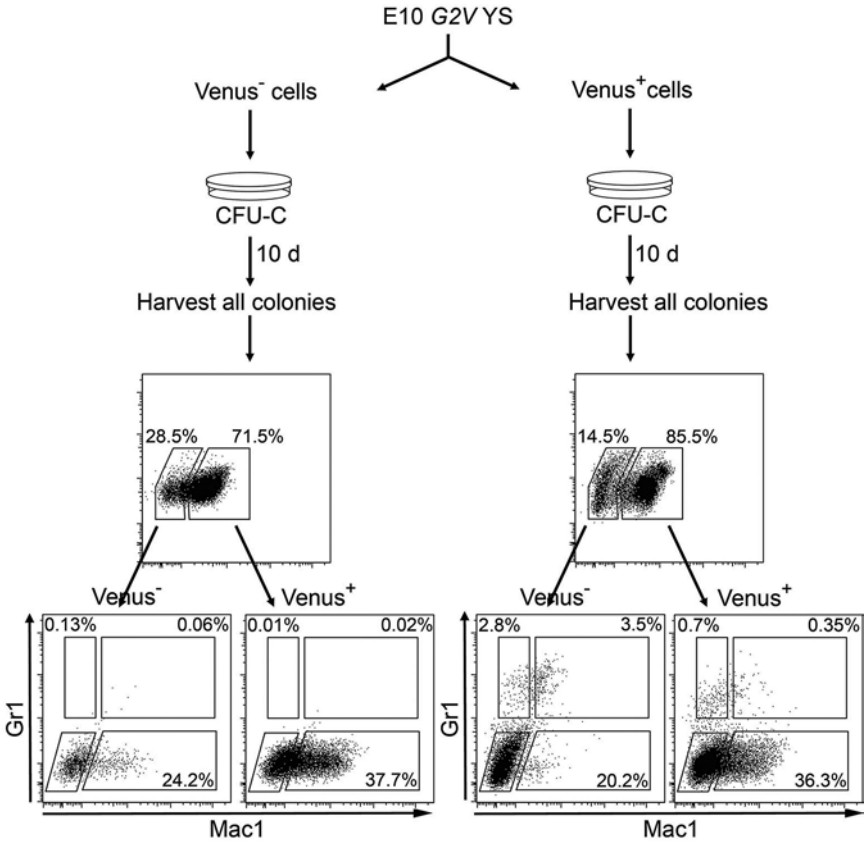
E10 G2V YS
Venus- cells
Venus+cells
CFU-C
CFU-C
10 d
10 d
Harvest all colonies
Harvest all colonies
28.5%
71.5%
14.5%
85.5%
Venus-
Venus+
Venus-
Venus+
0.13%
0.06%
0.01%
0.02%
2.8%
3.5%
0.7%
0.35%
Gr1
24.2%
37.7%
Gr1
20.2%
36.3%
Mac1
Mac1

Figure 7

Online Supplemental Methods

Gata2Venus ESC and mice. Gata2 homology arms were amplified with primers as specified in Supplemental Table 1 and cloned into TOPO (Invitrogen). An *IRES-Venus* fragment was inserted between left and middle, and *loxP-PGK-Puro-loxP* between middle and right arms in pSP72. IB10 ESCs were transfected with linearized vector (20μg), puromycin-selected and 360 clones PCR screened for *Gata2 Venus* (right arm junction – primers in Table1; 2292bp). Correct integration was verified by Southern blot (left arm) for 2 clones with normal karyotype. ESC+MEF were cultured in DMEM, 15%FBS, 1%Glutamax, 1%non-essential amino acids, 1%sodium pyruvate, 50μM βmercaptoethanol, 1000U/ml LIF at 37°C, 5%CO_2. Founders were identified by *Venus* PCR. First generation *G2V* offspring were crossed with *CAG-Cre* mice [22] and backcrossed (>10 generations) with C57BL/6.

Mice and embryo production. Gata2$^{+/-}$mice [5], Ly5.1 (6-8 week) and C57BL/6 mice were obtained/maintained (Harlan or locally) and genotyped by PCR. For PCR primers see Supplemental Table1. Day of plug discovery is embryonic day (E)0. Embryos were individually staged by somite pair (sp): E9=16-28sp, E10=28-40sp, early E10=28-34sp, E10.5=35-40sp, E11=40-50sp.

Immunostaining. Whole-mount conceptuses [23] were suspended in PBS/10%FCS, fixed in 2%PFA, and 100%MeOH. The trunk was dissected, anti-cKit and anti-CD31 stained, made transparent in 1:2BABB, and analysed (LeicaSP5) with Z-stack reconstructions (50–150μm) by LasAFsoftware. For cryosectioning [8] embryos were fixed in 2%PFA (20min), suspended in 20%sucrose O/N, snap-frozen in TissueTec, sectioned (HM630 cryostat) and fixed (acetone). Anti-CD34-biotin (1:50, BD), anti-Gata3 (1:10 clone KT122, 111207H09, Absea) and anti-Gata4 (1:50, sc-9053, SantaCruz) and anti-GFP antibodies O/N and secondary antibody incubation at RT, DAPI counterstained, mounted (Vectashield) and imaged (LeicaSP5). For flow cytometry, cell suspensions were made by collagenase treatment or direct dissociation and filtration [8], stained with anti-CD31 (390, BD), anti-CD34 (RAM34, BD), anti-cKit (2B8, BD), anti-CD41 (MWReg3, SantaCruz), anti-Sca1 (D7, Ebiosciences) and anti-CD16/32 (2.4G2, BD) antibodies, Hoechst 33258 (BD) and analysed on a FACSARIAIII/SORP.

Hematopoietic assays. Venus-sorted E9, E10, E11AGM, V+U, PL and YS and E10FL or *Gata2*-deficient E9-E10 AGM, V+U and PL (1 embryo equivalent (ee) of E9, E10 and E11 AGM, 0.1 ee V+U V^+, 0.1 ee PL V^+,0.1 ee YS V^-, 0.03 ee YS V^+ and 0.1 ee E10 FLs) were seeded in 3.6ml Methylcellulose (1ml per dish; M3434, StemCellTech)(or 0.9 and 0.1 ee of

Gata2$^{-/-}$ V+U and *Gata2*$^{-/-}$ YS 0.1 and 0.03 ee were seeded in 1.2 ml and distributed in a single dish) and cultured for 10-12 days[24]. Colonies were isolated, washed and Venus expression examined by FACSARIAIII/Fortessa. Sorted *G2V* E11AGM (Ly5.1/Ly5.2) cells were transplanted as described previously[24]. In short, AGMs were dissected and collagen II treated for 45 minutes. Subsequently dissociated and washed. When appropriate, the cells were stained and subsequently FACS sorted and collected in 50% FCS/ 50% PBS. Sorted *G2V* E11 AGM (Ly5.1/Ly5.2) cells were washed to PBS and injected into 9.5 Gy-irradiated (C57BL/6 x 129)F1 recipients (Ly5.2/Ly5.2) together with 2x10^5 spleen cells from the recipient strain. Peripheral blood (PB) donor chimerism was determined by *Venus* PCR or FACS at 1 and 4mo post-transplantation and scored positive if PB donor chimerism was >10% and multiorgan/lineage chimerism was >1%. For secondary transplantations, 3x10^6 BM cells from primary reconstituted recipients (4mo post-transplantation) were injected into 9.5 Gy-irradiated recipients and repopulation analysed at 4mo post-transplantation.

RNA analyses. E10.5 AGM cells were stained and sorted (CD31-PE-Cy7, 390, Biolegend; ckit-APC, 288, BD), washed, resuspended in RNAlater (LifeTechnologies) and stored at −20°C. RNA preparation was with mirVana miRNA Kit (Ambion) and quality/quantity were assessed on a 2100 bioanalyzer (Agilent Technologies) with a RNA Nano/Pico chip. RNAsequencing used SMARTER protocol for Illumina HiSeq2000. Sequences were mapped to mouse (version 10) and FPKMs calculated using TopHat (v2.0.13) and Cufflinks (v2.2.1) with fragment-bias and multi-read corrections[25]. Expression difference threshold was >2-fold change and higher or lower expressing genes were applied to Enrichr tool. Enrichr output (and calculated p-values from Chi2 tests) were imported into R and corrected for multiple testing (FDR) and a threshold of FDR <0.05 was used. For GSEA, ratios were calculated for AGM CD31$^+$c Kit$^+$Venus$^-$ versus CD31$^+$cKit$^+$Venus$^+$ FPKMs(+1) and used with GSEA (version2.2.0) preranked method using default options[26,27]. GEO Data Accession Number is GSE76254.

For qRT-PCR, SuperScriptII or III ReverseTranscriptase (LifeTechnologies) was used for first-strand cDNA synthesis. Reaction mix=0.2µM forward (F) and reverse (R) primers, 2µl cDNA, 0.2mM nucleotides and 1U Platinum®*Taq* Polymerase (LifeTechnologies) with 30-40 cycles (Bio-Rad rtPCRThermocycler): with primers as described in supplementary table 1. *β-actin* was used for normalization.

Supplemental Table 1. Primer sequences

Cloning	Fwd	Rev
left	5'AATCGATGCCGAGGGAGTTCAGTGCTAG 3'	5'AGATATCACAGTAATGGCGGCACAAGGC3'
right	5'ATACGTACAGGAAGGAAACATTCTCTGG3	5'ACTCGAGGTCTCAGGCAAGACTATGG3'
middle	5'CATATGGCCTGGAATCTGCGCAGGAC3'	5'GCGGCCGCAATATTTCTAACTGGGCTGC3'
Genotyping		
right arm junction	5'CAGCTTCAGCCTGCTTACTCA3'	5'TATAGACAAACGCACACCGGC3'
Gata2$^{-/-}$	GGAACGCCAACGGGGAC	GCTGGACATCTTCCGATTCCGGGT
qRT-PCR		GATCTCCTGTCATCTCACCTTGCT
Venus	F5'ATCTTCTTCAAGGACGACGG3'	R5'GGCTGTTGTAGTTGTACTCC3'
Gata2	F5' AAGCTGCACAATGTTAACAGG3'	R5'CCTTTCTTGCTCTTCTTGGAC3'
Gata1	F5'TGCCTGTGGCTTGTATCA3'	R5'TGTTGTAG GGTCGTTTGAC3'
Gata3	F5'CCTTATCAAGCCCAAGCGA3'	R5'GATGCCTTCTTTCTTCATAGTCAG3'
Gata4	F5'GAGCTGGTGCTACCAAGAGG3'	F5'GAGCTGGTGCTACCAAGAGG3'
Gata5	F5'CGACGTAGCCCCTTCGTGG3'	R5'GCCACAGTGGTGTAGACAG3'
Gata6	F5'GCCTGCGGCCTCTACATGAA3'	R5'CAGGACCTGCTGGCGTCTTA3'

Supplemental Figure 1

Representative multilineage FACS analysis of GataVenus$^+$ repopulated recipients. Recipients repopulated with Venus$^+$ cells from *G2V* E11 AGM were examined at 4mo post-transplantation for donor-derived cells. Bone marrow (BM), spleen, lymph node (LN), peripheral blood (PB) and thymus cells were isolated and examined for the Ly5.1 donor marker in multiple lineages. (Top panel) BM viable cells were gated into the following fractions - CD31$^+$Gr$^-$ =lymphoid; CD31$^-$Gr1$^-$ =erythroid; CD31$^+$Gr1$^+$ and CD31$^-$Gr1$^+$ =myeloid. (Second row panels) percentages of Ly5.1 (Y-axis) cells in gated erythroid, lymphoid and myeloid lineage fractions are indicated. (Third row, Left panel) Spleen viable cells were gated on B cells (B220$^+$) and T cells (CD4$^+$/CD8$^+$) and (Right panels) show percentages of Ly5.1 (Y-axis) donor-derived B and T cells. (Bottom row panels) Percentages of Ly5.1 donor-derived cells are shown for viable cells from LN, PB and Thymus. X-axis is side scatter (SSC-A) in all Ly5.1 plots.